

# Using harmonic analysis of green LAI time series obtained from Sentinel-2 imagery for daily representation of crop growth in a hydro-agroecological model

LUKAS GRAF<sup>1</sup>, ISABELLA KAUSCH<sup>1</sup>, HEIKE BACH<sup>1</sup> & TOBIAS HANK<sup>2</sup>

*Abstract: Harmonic Analysis of Time Series (HANTS) was used to obtain daily reconstructed values of green leaf area index (GLAI) from optical Sentinel-2 imagery for a maize and a winter wheat field plot in Southern Germany in order to represent crop growth in the hydro-agroecological PROMET model. Daily GLAI time series were retrieved with high accuracy in case of winter wheat ( $R^2=0.90$ ,  $RMSE=0.78 \text{ m}^2/\text{m}^2$ ) and slightly lower accuracy in case of maize ( $R^2=0.85$ ,  $RMSE=1.05 \text{ m}^2/\text{m}^2$ ) from the imagery by radiative-transfer model inversion. Assimilating these reconstructed GLAI time series into PROMET using the model forcing technique allowed for retrieving winter wheat fruit biomass ( $R^2=0.98$ ,  $RMSE=0.08 \text{ kg}/\text{m}^2$ ) as well as maize above-ground biomass ( $R^2=0.97$ ,  $RMSE=0.12 \text{ kg}/\text{m}^2$ ) with considerable high accuracy. The proposed approach offers opportunities for contiguous crop growth monitoring as well as biomass and yield modelling.*

## 1 Introduction

To tackle the rapidly growing demand for food and biomass, the contiguous monitoring of crop growing conditions was announced by the „Group on Earth Observations“ (GEOS) as one of the keystones of applied Earth Observation (LAUTENBACHER 2006).

Green leaf area index (GLAI) is a dimensionless biophysical variable that is defined as the one-sided area of green leaves per ground unit. It describes the surface area available for the exchange of mass and energy between plants and the atmosphere and therefore is often used for assessing crop development over the growing cycle (MADDONI & OTEGUI 1996). Time series of GLAI derived from optical satellite imagery provide essential information about crop growing conditions for wider areas. This information can be employed to augment physically-based land surface models that simulate the growth of plants according to fluxes of mass and energy.

HANK et al. (2015) have shown that the assimilation of GLAI values derived from optical high resolution satellite data using radiative transfer models improves the accuracy of the agro-ecological PROMET model by enhancing spatial detail and proving spatially continuous parametrization of crop growing conditions. The time-step of PROMET simulations is one hour, which allows for a highly dynamic representation of diurnal and inter-diurnal crop development based on physical constraints. While the strengths of agro-ecological models like PROMET lie in their generic spatial modelling capacity and high temporal resolution, crop parameters derived from optical satellite imagery, e.g. from Sentinel-2, can be used to re-initialize model runs based on concurrent observations of crop growing conditions to allow for more accurate yield forecasting

---

<sup>1</sup> VISTA Geowissenschaftliche Fernerkundung GmbH, Gabelsbergerstraße 51, D-80333 München, E-Mail: [graf, kausch, bach]@vista-geo.de

<sup>2</sup> Ludwig-Maximilians-Universität München, Department für Geographie, Luisenstraße 37, D-80333 München, E-Mail: [tobias.hank]@lmu.de

and related aspects of agro-ecological modelling (DORIGO et al. 2007). In order to ensure high modelling accuracy, data availability of satellite imagery is a critical aspect, as data assimilation usually often occurs within relatively small time-steps.

Although Sentinel-2 provides a very high temporal resolution with revisit times of up to five days due to the twin constellation of Sentinel-2A and 2B, time series of GLAI derived by inverting radiative transfer models still suffer from data gaps and outliers due to undetected cloud shadows and adjacency effects. Thus, GLAI values cannot be provided on a daily base. In order to overcome these data gaps HANK et al. (2015) developed a methodology of stepwise crop growth simulation using different scenarios of model parameters. Whenever a satellite observation allows for an update of the GLAI values, the model is reinitialized from the last EO assimilation time step to the newest one using the best fitting scenario. This procedure is producing yield maps that correlate strongly with maps from combines (MIGDALL et al. 2009), however the workflow is complex and the computational time high. Therefore it would be considered optimal to use daily GLAI values for assimilation into the PROMET model in order to allow for continuous model forcing instead of stepwise updating.

In order to address this issue, the use of the Harmonic Analysis of Time Series (HANTS) algorithm is proposed (ROERINK et al. 2000). HANTS is capable to, firstly, detect and remove outliers from a time series and, secondly, to decompose a time series into its harmonic components, thereby allowing for the reconstruction of missing values. While HANTS was shown to return accurate results in a broad range of remote sensing domains, including the reconstruction of NDVI time series (JAKUBAUSKAS et al. 2001; ROERINK et al. 2000; ZHOU et al. 2015) and land surface temperature time series (XU & SHEN 2013) as well as the characterisation of land surface types (JAKUBAUSKAS & LEGATES 2000), only a relatively small number of studies has investigated the reconstruction of LAI time series (for instance TUM et al. 2016). Furthermore, to our knowledge, only little efforts have been undertaken to study the use of reconstructed GLAI time-series in agro-ecological models.

Therefore, the objectives of this study were twofold: Firstly, the retrieval accuracy of remote sensing derived GLAI time-series processed by the HANTS algorithm was investigated by comparing the daily outcomes of the HANTS algorithm with in-situ measurements for winter wheat (*Triticum aestivum*) and maize (*Zea mays*) for a test-site in Southern Germany. Secondly, crop biomass values obtained from PROMET simulations with assimilated HANTS-processed GLAI data were compared to field measurements.

The structure of this paper is based upon those objectives: In the first section a brief overview of the used data and the study area is provided. In the second section the workflow and methods are described in more detail while the results are presented and discussed in the third part of this paper.

## 2 Data and Study Area

In this study, multi-spectral Sentinel-2 imagery in L1B processing level was acquired from Copernicus Scientific Data Hub (<https://scihub.copernicus.eu/>). Sentinel-2, with its high spatial resolution (10m) as well as with its enhanced spectral band settings, has shown promising results in the retrieval of LAI and related biophysical plant parameters (ATZBERGER & RICHTER 2012; RICHTER et al. 2012). Moreover, its twin constellation allows for the monitoring of plant growing

conditions with high temporal resolution. This high temporal resolution is an essential prerequisite for providing operational monitoring services like GEOGLAM (<http://geoglam.org/index.php/en/>) that aim for contiguous global crop growth monitoring.

To allow for monitoring a whole growing period, 40 cloud-free Sentinel-2 scenes were downloaded for a study area located north of Munich (Germany). The study site covered two agricultural fields, one cultivated with winter wheat and one with maize. The fields were regularly monitored by in-situ measurements of LAI and related leaf and canopy parameters between 1<sup>st</sup> March and 31<sup>st</sup> August 2018 (Fig. 1). Twelve field sampling dates at nine neighbouring points were available in case of maize, whereas ten field sampling dates at nine neighbouring points were used in case of winter wheat. Each of the sampling points accounts for exactly one adjacent Sentinel-2 pixel in 10m spatial resolution as can be derived from Fig. 1.

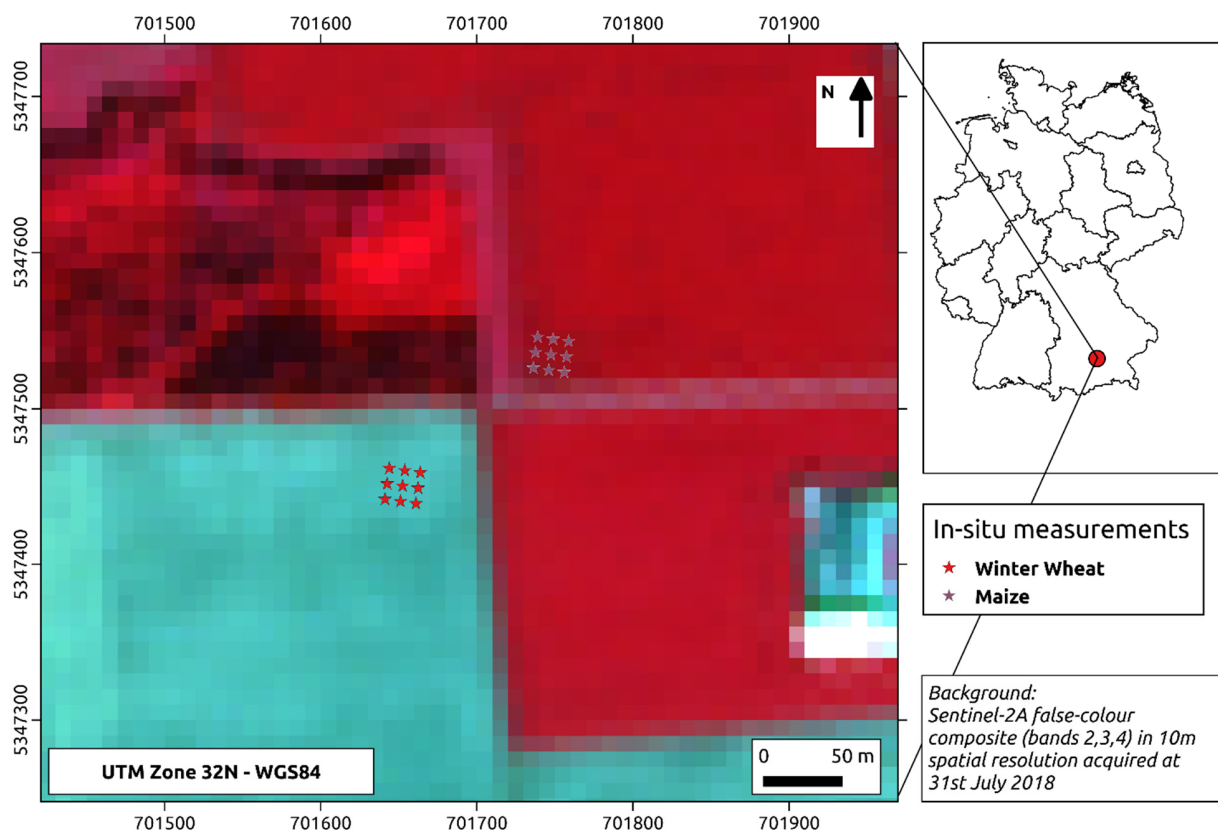


Fig. 1: Overview map showing the location of the study area north of Munich (Germany) and the position of the winter wheat (green) and maize (purple) sampling plots that were examined in this study. In the background a false-colour composite (bands 8, 4, 3) of a Sentinel-2A scene acquired on 31st July 2018 in 10m spatial resolution is displayed.

All in-situ LAI measurements were conducted using a LI-COR LAI 2200C Plant Canopy Analyser (LI-COR Inc.) that provides non-destructive estimates of total LAI. GLAI was computed from these measurements by multiplying the total LAI with the fraction of brown leaves that was estimated during the field visits. Besides GLAI measurements, crop biomass values were acquired destructively. Avoiding disturbance of the continuous non-destructive measurements, the destructive biomass sampling was conducted at adjacent points located in the same field plots. The

biomass samples thus represent locations which were subjected to identical management measures as the points where GLAI was non-destructively obtained.

The selected study area (Fig. 1) reflects a highly-intensified agricultural region, thereby accounting for characteristic farm management measures in terms of fertilizer utilization and nutrient supply. Considering the 1961-1990 records, the study area is dominated by humid conditions (annual precipitation about 810mm) and moderate air temperatures (average temperature 2m above ground about 9.0°C) which are typical for mid-latitude geographic regions characterized by a warm-temperate climate. Precipitation and air temperature in 2018 differed notably from average conditions as the months between April and August 2018 were exceptionally warmer and drier compared to the long-term average (years 1961 to 1990) as indicated by a nearby agrometeorological weather station in Weißenstephan operated by the Bavarian State Research Centre for Agriculture (LfL Bayern).

### 3 Methods

#### 3.1 Green LAI retrieval from Sentinel-2 imagery

The acquired Sentinel-2 imagery was converted to surface reflectance values using an approach proposed by VERHOEF & BACH (2003) making use of the MODTRAN (moderate resolution atmospheric transmission) model taking into account atmospheric conditions as well as adjacency effects. To ensure comparable geolocation all scenes were checked for systematic shifts in their x- and y-coordinates to avoid geometrically distorted time series.

First of all, the obtained surface reflectance values were used to run the Soil-Leaf-Canopy (SLC) radiative transfer model (VERHOEF & BACH 2007) in inverse-mode. SLC is a physically-based model that is based on a four-stream radiative transfer approach to account for direct and diffuse fluxes of incident and reflected radiation depending on biophysical as well as biochemical plant parameters and the properties of the underlying soil. Several studies demonstrated the potential of SLC to accurately derive plant parameters for agricultural purposes (MIGDALL et al. 2009; VERHOEF & BACH 2007).

As the inversion of radiative transfer models cannot be done analytically a numerical approach using a Lookup-table (LUT) was established. For each scene and each of the both crop types a LUT was compiled containing plant specific parameters and the current viewing and illumination conditions. Plant parameters were adapted parallel to the phenological development of the crops (expressed as BBCH growth stages) to account for changes of crop physiology and chemistry over the growing period.

During the inversion process, satellite-derived spectra were compared to the spectra stored in the LUT. The Root Mean Squared Error (RMSE) criterion thereby was used as cost function. The synthetic spectrum with the smallest RMSE provided then the GLAI value of a certain pixel. If the RMSE of the matching spectra exceeded a threshold of 2% (expressed as reflectance values) the result of the inversion was flagged as of poor quality and not included into the time-series stack of GLAI values.

### 3.2 Outlier removal and reconstruction of missing values using HANTS

The obtained GLAI time-series were processed by the HANTS algorithm (ROERINK et al. 2000) using a number of three frequencies. The number of frequencies was predetermined through a Fourier analysis by assessing the number of dominant frequencies in the frequency domain. These frequencies were used to decompose a periodic signal – such as GLAI time-series – expressed by an analytic function  $f(t)$  (Eq. 1) into its harmonic components  $\gamma$  and an error term  $\varepsilon$  in an iterative manner.

$$f(t) = \gamma + \varepsilon \quad (\text{Eq. 1})$$

Thereby iterative least square fitting was employed to minimize the error term according to the workflow proposed by JAKUBAUSKAS et al. (2001).

The harmonic components (also referred to as harmonic terms) are mathematically expressed as a superposition of sines and cosines characterized by different frequencies and amplitudes. Data points showing deviations too large from the harmonic terms are removed in each iteration until the number of maintained data points drops below a predefined minimum number of valid observations or a user-defined error-tolerance threshold is exceeded. After each iteration, the harmonic terms are recomputed based on the remaining data points. As a consequence, HANTS is capable to remove outliers from time-series and to restore GLAI values in user-defined equidistant temporal units (e.g. days).

In this study, for each time-series a minimum of nine valid data points was imposed to ensure that the results of HANTS were mathematically robust. Iteration was stopped when the number of valid observations dropped below the minimum number or an error convergence criterion was met. This criterion - expressed as the deviation between the remaining original data points and the fitted harmonic curve - was met when the overall error between the original and reconstructed GLAI values dropped below  $1.0 \text{ m}^2/\text{m}^2$ . The resulting harmonic curve providing GLAI values on a per-day basis was then post-processed to remove possible over- or undershooting that would cause unrealistic representation of crop development. Using the daily reconstructed values, a comparison to field measurements was undertaken in order to investigate whether the retrieval accuracy of GLAI met the criterion of 10% relative accuracy expressed as Normalized RMSE as proposed by the Sentinel mission requirements (ESA 2007).

### 3.3 Assimilation into the PROMET model

Finally, the reconstructed time-series of GLAI were used to update the agro-ecological PROMET by assimilating the satellite-derived observations into the model (HANK et al. 2015). As PROMET is a raster-based model, assimilation is facilitated by using inter-changeable (artificial) spatial units that are called “proxel” in PROMET and pixel in image analysis. PROMET solves physical equations describing the exchange of mass and energy for each spatial unit hourly. Consequently, GLAI as a canopy variable is provided by PROMET for each spatial unit for every single hour.

Assimilation of remotely sensed derived GLAI values into PROMET usually follows one of the three approaches proposed by DELÉCOLLE et al. (1992): Model calibration, parameter updating and model forcing. While the two former assimilation methods do not require continuous input of remote sensing data these approaches cause either large computational efforts in case of parameter updating or physically implausible crop growth simulation by introducing sharp steps in case of

model updating. Model forcing, in contrast, drastically reduces computational efforts by forcing PROMET to follow a given continuous GLAI time series as provided by HANTS.

Crop biomass development was then modelled by PROMET using model forcing over the whole growing period and compared to in-situ measurements in order to quantify crop growth modelling accuracy. Herein, a distinction between maize and winter wheat was made as for maize silage the whole above ground biomass including leaves and stems is usually harvested while in case of winter wheat the fruits (grains) are the most important compartment of the crop.

## 4 Results and Discussion

### 4.1 Analysis of GLAI time-series plots

The Sentinel-2 derived time series of GLAI covering the whole crop growing season are displayed for a single ground point in Fig. 2a) and 2b) for maize and winter wheat, respectively. For each time-series the HANTS interpolated values (solid black line), the removed outliers (red dots), the remaining remotely sensed derived values (green dots) as well as the in-situ measured GLAI values (blue dots) were shown.

Generally, all time-series followed an expected temporal pattern of GLAI development starting from values near zero LAI at the beginning of the crop growing period. After seeding, the plants started accumulating biomass and subsequently GLAI increased until a peak around August (maize) and June (winter wheat) was reached. After reaching these peaks, GLAI values declined within a relatively short time interval as the plants matured and green plant pigments were disintegrated. At the end of the observed growing period (harvest) GLAI values were near zero again. Therefore, the HANTS-reconstructed time-series can be considered as physically meaningful. Apart from that, a plateau-like pattern between begin of July and end of August could be identified from the in-situ data for maize (Fig 2a) indicating that GLAI development stagnated during this time period.

In more detail, the time-series plot of maize (Fig. 2a) contained a large amount of removed outliers that were identified from the remotely sensed derived GLAIs. The outliers were partly related to relatively low values during the summer period (July to September) that could be caused by cloud shadows. Additionally, very high GLAI values ( $> 5 \text{ m}^2/\text{m}^2$ ) derived during August were marked as outliers. The plateau-like pattern, however, was not completely captured by the HANTS-reconstructed GLAI curve as some of the rejected GLAI values were quite close to the corresponding in-situ measurements. Furthermore, within the plateau-like feature the in-situ measurements indicated the presence of relatively high frequencies as GLAI values showed de- and increases within short time periods. Consequently, the HANTS derived curve reflected absolute values of GLAI fairly accurately but did not completely capture the high frequent dynamics present in the in-situ measurements.

In case of winter wheat (Fig. 2b) the derived time series revealed high agreement between the HANTS reconstructed curve and the in-situ measured values. Moreover, the amount of removed outliers was lower as only five outliers within this particular time-series could be identified. These outliers were characterized by clearly lower satellite-derived GLAI values compared to the in-situ measurements. Consequently, the HANTS derived curve quite accurately reflected the temporal

pattern expected from the in-situ measurements in terms of temporal dynamics and absolute values.

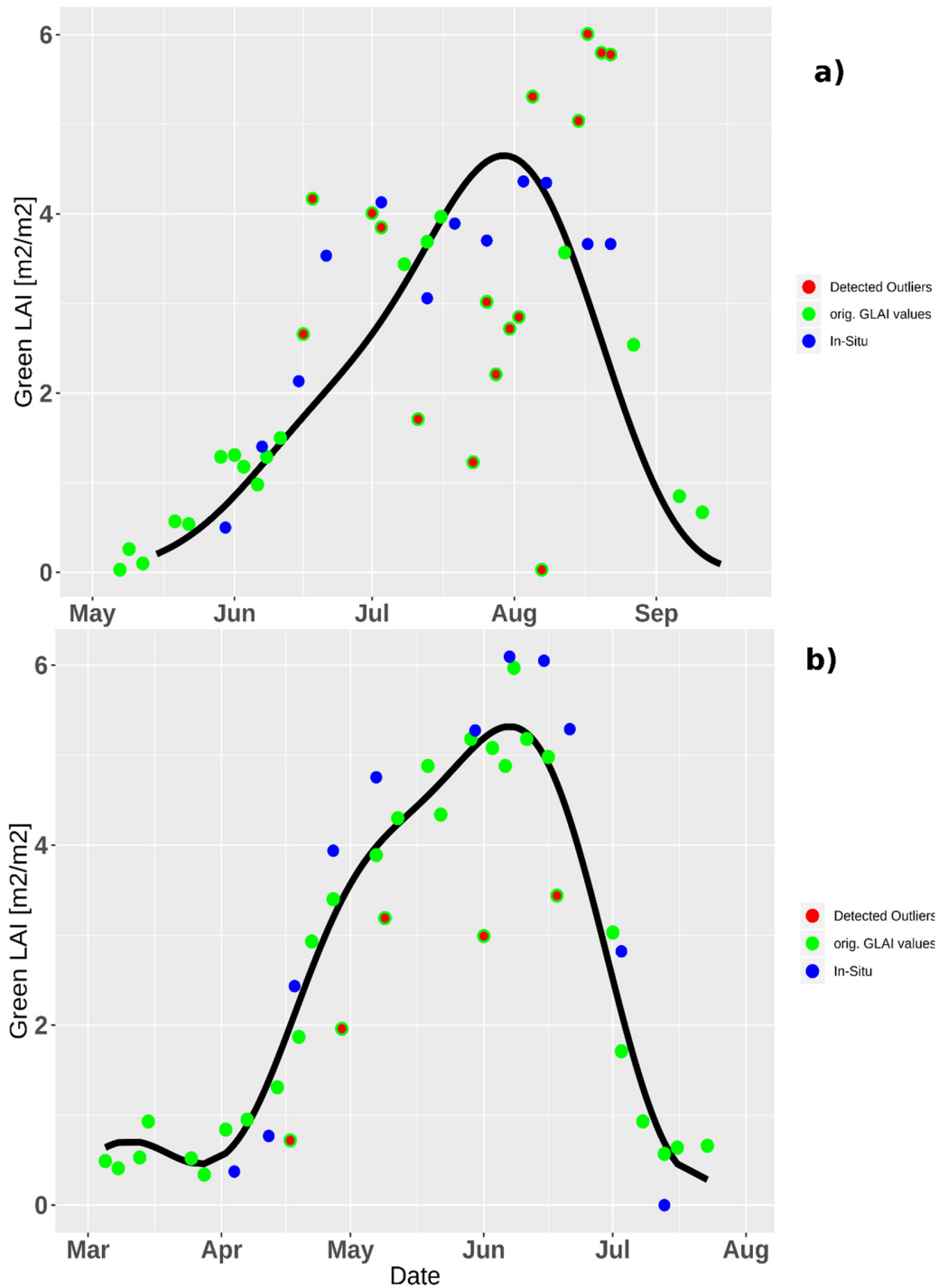


Fig. 2: Time series of green LAI values obtained from point number one of maize (a) and winter wheat (b) showing the HANTS reconstructed daily values (solid line), the removed outliers (red dots), the remaining remotely sensed derived values (green dots) and the in-situ measurements (blue dots).

## 4.2 Analysis of scatter plots of GLA

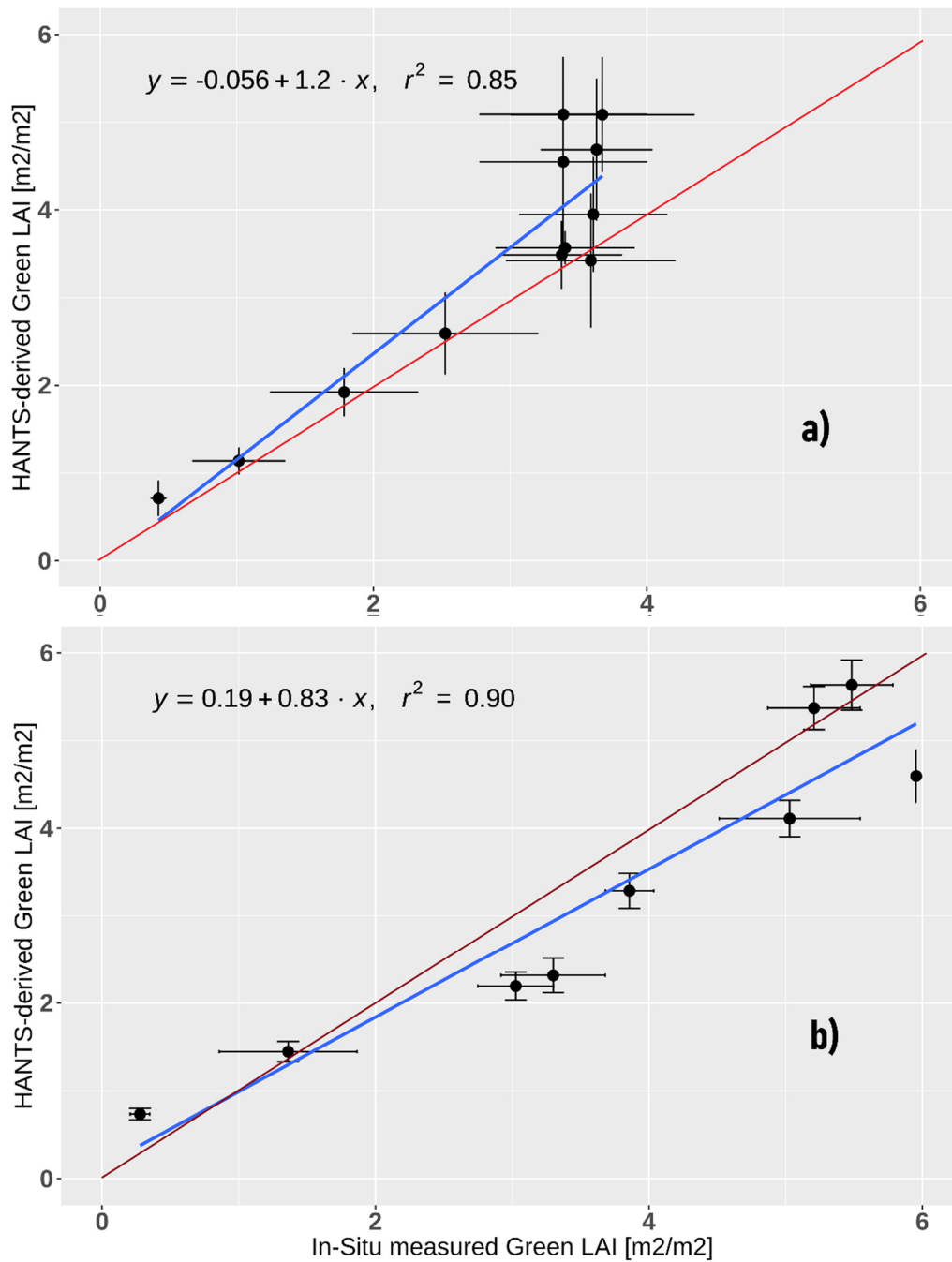


Fig. 3: Scatter plots of in-situ vs. HANTS-derived GLAI values based on the spatial average of all nine points per crop type showing maize (a) and winter wheat (b). Vertical and horizontal bars indicate the standard deviation of HANTS-derived and in-situ values, respectively. The one-to-one fit is displayed as red line.

Besides these assessments, scatter plots based on a spatial average of all nine points for both crop types (see Fig. 1) for all dates with in-situ measurements were plotted to compare HANTS-derived



GLAI values against in-situ measurements (Fig. 3). The solid red line indicates the desired one-to-one relationship. In Fig. 3, for each date the spatial average together with the standard deviation (SD) of the in-situ measured (horizontal bars) and the HANTS-derived values (vertical bars) is shown to account for the observed spatial variation within the two field plots.

In case of maize (Fig. 3 a) HANTS-derived values were in considerable agreement to in-situ measured GLAIs resulting in  $R^2 = 0.85$  and a RMSE of  $1.05 \text{ m}^2/\text{m}^2$ . As shown by the vertical and horizontal bars in Fig. 3 a SD was up to  $\pm 0.5 \text{ m}^2/\text{m}^2$  green LAI indicating a relatively high degree of spatial variation for each date. Normalized RMSE (NRMSE) was 37.5% that exceeded the desired accuracy of 10%.

The relatively high NRMSE for maize could be either related to an inaccurate parametrization of maize within the SLC model or to an inappropriate setting of the parameters used within HANTS (e.g. inappropriate number of frequencies). Furthermore, in multi-temporal model inversion processes, as presented in this study, phenological stages of the crop growing cycle are determined by a distinct set of leaf and canopy parameters that change over the time. If extreme weather conditions like during summer 2018 cause phenological patterns that differ significantly from average conditions it is feasible to assume that the model parametrization did not completely capture derivations from the usual crop growing cycle. Especially the stagnation of GLAI development during the summer months (see Fig. 2a) was not well captured by the HANTS reconstructed curve. This finding could explain the deviation between in-situ measured and HANTS-derived GLAI values.

Regarding winter wheat, the relationship between HANTS-derived and in-situ measured GLAI came close to the one-to-one line (red line) as also indicated by a high  $R^2$  (0.90) and a low RMSE ( $0.78 \text{ m}^2/\text{m}^2$ ). The NRMSE was about 12.2%, thus almost reaching the targeted accuracy of 10%, and was in good agreement to results of recent studies on GLAI retrieval from optical satellite data (DUVEILLER et al. 2011, ALI et al. 2015).

### 4.3 Crop Growth Modelling Accuracy

In-situ measured and PROMET-simulated crop biomass values acquired during the growing period were plotted in Fig. 4 showing the development of leaf, stem, fruit (grain) and overall above ground biomass over time for maize (Fig. 4a) and of leaf and fruit biomass for winter wheat (Fig. 4b).

In general, all curves of biomass development followed an expected temporal pattern: Fruit biomass accumulated over the growing period and reached a maximum at the time of harvest (begin of September and mid of July for maize and winter wheat, respectively). Leaf and stem biomass, in contrast, reached their maximum earlier (begin of August and begin of June, respectively) and declined afterwards as plants matured.

In case of maize (Fig. 4a) overall above ground biomass was simulated with fairly high accuracy when compared to in-situ measurements ( $R^2=0.97$ ,  $\text{RMSE}=0.12 \text{ kg}/\text{m}^2$ ). The NRMSE was about 15.0% thus coming quite close to the targeted accuracy of 10%. As for maize silage the overall above ground biomass is usually harvested completely, the results reveal promising opportunities for maize yield modelling. Furthermore, the potential of the proposed approach for continuous monitoring of maize growing conditions was demonstrated as PROMET was capable to model biomass development over the whole growing period for all crop compartments.

Regarding winter wheat (Fig. 4b), fruit (=grain) biomass was simulated with considerable accuracy ( $R^2=0.98$ ) resulting in a RMSE value of  $0.08 \text{ kg/m}^2$ . NRMSE was about 24.2% that exceeded the targeted accuracy of 10%. At the time of harvest (13<sup>th</sup> July), however, the relative error between measured and simulated fruit biomass was about 10.6% thus fulfilling the accuracy requirements at the usually most important stage of crop growth modelling. In addition, the temporal patterns of crop development simulated by PROMET showed an overall good agreement to the in-situ measurements. Thus, the proposed approach seems to be capable for contiguous winter wheat growth monitoring as well as yield forecasting.

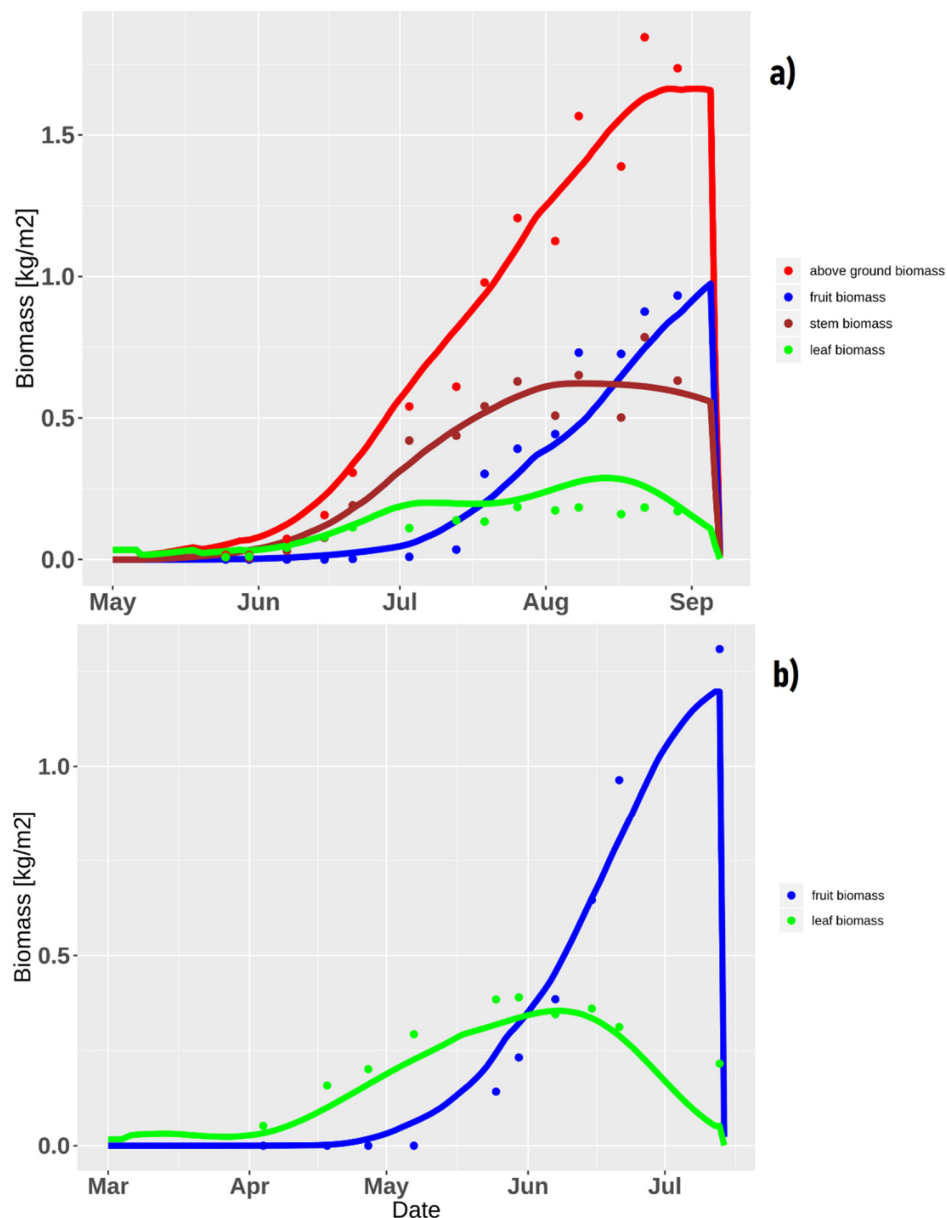


Fig. 4: Time series plot of above ground (red), fruit (blue), stem (brown) and leaf (green) biomass showing PROMET-simulated (solid lines) and in-situ measured (dots) values for maize (a) and winter wheat (b). For winter wheat only fruit and leaf biomass were assessed.

## 5 Conclusions and Outlook

The presented results indicate the potential of assimilating daily re-constructed GLAI values into the process-based agro-ecological PROMET model using the HANTS algorithm. HANTS was capable to provide physically meaningful and accurate curves of daily GLAI development that could be used for computational efficient model forcing assimilation techniques. PROMET simulations allowed to retrieve crop biomass with high accuracy over the whole growing cycle thereby offering opportunities for continuous crop growth monitoring and yield estimation.

In the future, the usage of HANTS should be extended from the single-pixel level to entire agricultural fields or even wider areas to assess its capacity in an operational context. By doing so, the impact of daily reconstructed GLAI values on crop biomass modelling could be discussed with regard to spatial variability – an essential aspect in site-specific precision farming - that can be hardly completely captured by the presented single-point considerations.

## 6 Acknowledgement

This study was carried out within the VirtualWaterValues (ViWA) project. ViWA is a collaborative project of the funding program "Global Resource Water (GROW)" in the framework program FONA (Research for Sustainability) of the German Ministry for Education and Research (BMBF) under grant code 02WGR1423A. In-situ data were collected as part of the research project "EnMAP Scientific Advisory Group Phase III Developing the EnMAP Managed Vegetation Scientific Processor", supported by the Space Agency of the German Aerospace Center (DLR) through funding by the German Federal Ministry for Economic Affairs and Energy under the grant code 50EE1623.

## 7 Literature

- ALI, M., MONTZKA, C., STADLER, A., MENZ, G., THONFELD, F. & VERECKEN, H., 2015: Estimation and Validation of RapidEye-Based Time-Series of Leaf Area Index for Winter Wheat in the Rur Catchment (Germany). *Remote Sensing*, **7**, 2808-2831.
- ATZBERGER, C. & RICHTER, K., 2012: Spatially constrained inversion of radiative transfer models for improved LAI mapping from future Sentinel-2 imagery. *Remote Sensing of Environment*, **120**, 208-218.
- DELÉCOLLE, R., MAAS, S., GUERIF, M. & BARET, F., 1992: Remote sensing and crop production models: present trends. *ISPRS Journal of Photogrammetry and Remote Sensing*, **47**(2-3), 145-161.
- DORIGO, W.A., ZURITA-MILLA, R., WIT, A.J.W. DE & BRAZILE, J., 2007: A review on reflective remote sensing and data assimilation techniques for enhanced agroecosystem modeling. *International Journal of Applied Earth Observation and Geoinformation*, **9**, 165-193.
- DUVEILLER, G., WEISS, M., BARET, F. & DEFOURNY, P., 2011: Retrieving wheat Green Area Index during the growing season from optical time series measurements based on neural network radiative transfer inversion. *Remote Sensing of Environment*, **115**, 887-896.

- EUROPEAN SPACE AGENCY (ESA), 2007: GMES: Sentinel-2 Mission Requirements Document, issue 2 revision 0-30/01/2007. 1-13.
- HANK, T.B., BACH, H. & MAUSER, W., 2015: Using a remote sensing-supported hydro-agroecological model for field-scale simulation of heterogeneous crop growth and yield: Application for wheat in central Europe. *Remote Sensing*, **7**, 3934-3965.
- JAKUBAUSKAS, M.E. & LEGATES, D.R., 2000: Harmonic analysis of time-series AVHRR NDVI data for characterizing us great plains land use/land cover. *International Archives of Photogrammetry and Remote Sensing*, **33**, 384-389.
- JAKUBAUSKAS, M.E., LEGATES, D.R. & KASTENS, J.H., 2001: Harmonic Analysis of Time-Series AVHRR NDVI Data. *Photogrammetric Engineering and Remote Sensing*, **67**(4), 461-470.
- LAUTENBACHER, C.C., 2006: The Global Earth Observation System of Systems : Science Serving Society. *Space Policy*, **22**, 8-11.
- MADDONI, G.A. & OTEGUI, M.E., 1996: Leaf area, light interception, and crop development in maize. *Field Crops Research*, **48**, 81-87.
- MIGDALL, S., BACH, H., BOBERT, J., WEHRHAN, M. & MAUSER, W., 2009: Inversion of a canopy reflectance model using hyperspectral imagery for monitoring wheat growth and estimating yield. *Precision Agriculture*, **10**(6), 508-524.
- RICHTER, K., HANK, T.B., VUOLO, F., MAUSER, W. & D'URSO, G., 2012: Optimal Exploitation of the Sentinel-2 Spectral Capabilities for Crop Leaf Area Index Mapping. *Remote Sensing*, **4**, 561-582.
- ROERINK, G.J., MENENTI, M. & VERHOEF, W., 2000: Reconstructing cloudfree NDVI composites using Fourier analysis of time series. *International Journal of Remote Sensing*, **21**(9), 1911-1917.
- TUM, M., GÜNTHER, K.P., BÖTTCHER, M., BARET, F., BITTNER, M., BROCKMANN, C. & WEISS, M., 2016: Global Gap-Free MERIS LAI Time Series (2002 – 2012). *Remote Sensing*, **8**, 1-19.
- VERHOEF, W. & BACH, H., 2007: Coupled soil-leaf-canopy and atmosphere radiative transfer modeling to simulate hyperspectral multi-angular surface reflectance and TOA radiance data. *Remote Sensing of Environment*, **109**, 166-182.
- VERHOEF, W. & BACH, H., 2003: Remote sensing data assimilation using coupled radiative transfer models. *Physics and Chemistry of the Earth*, **28**(Parts A/B/C), 3-13.
- XU, Y. & SHEN, Y., 2013: Reconstruction of the land surface temperature time series using harmonic analysis. *Computers & Geosciences*, **61**, 126-132.
- ZHOU, J., JIA, L. & MENENTI, M., 2015. Reconstruction of global MODIS NDVI time series : Performance of Harmonic Analysis of Time Series (HANTS). *Remote Sensing of Environment*, **163**, 217-228.